Published in final edited form as:
Free Radic Biol Med. 2010 December 15; 49(12): 2078–2087. doi:10.1016/j.freeradbiomed.2010.10.691.

Thioredoxin 1 as a subcellular biomarker of redox imbalance in human prostate cancer progression

Weihua Shan[1,2], **Weixiong Zhong**[2,3], **Rui Zhao**[4], and **Terry D. Oberley**[1,2,3]

[1] Molecular and Environmental Toxicology Center, University of Wisconsin, School of Medicine and Public Health, Madison, WI 53705

[2] Department of Pathology and Laboratory Medicine, University of Wisconsin School of Medicine and Public Health, Madison, WI, 53705

[3] Pathology and Laboratory Medicine Service, William S. Middleton Veterans Memorial Hospital, Madison, Wisconsin 53705

[4] Department of Comparative Biosciences, School of Veterinary Medicine, Madison, WI, 53706

Abstract

We determined protein levels and subcellular distribution of thioredoxin 1 (Trx1) in human prostate tissues using tissue microarrays and analyzed redox changes of Trx1 in the nucleus and cytoplasm in cell culture models with redox western blot technique. We demonstrated increased nuclear Trx1 levels in high- versus low-grade human prostate cancers. Despite increased protein levels, the oxidized forms of nuclear Trx1 were higher in prostate cancer cell lines compared to their benign counterparts, suggesting that nuclear redox imbalance occurred selectively in cancer cells. A growth-stimulating dose of androgen caused transient oxidation of Trx1 in androgen-responsive prostate cancer cells only, suggesting a loss of both androgen- and redox-signaling mechanism during cancer progression. Androgen-independent PC3 cells showed a significant increase in nuclear and cytoplasmic Trx1 protein levels, but a significant decrease in total Trx activity. Trx1 redox states and activity, correlated with the sensitivity of prostate cancer cells to prooxidant agents, and downregulation of Trx1 sensitized cancer cells to these agents. Our findings suggest that loss of Trx function due to oxidation and corresponding redox imbalance may play important roles in prostate cancer progression and response to therapies; and Trx1 may serve as a biomarker of subcellular redox imbalance in prostate cancer.

Keywords

Thioredoxin 1; reactive oxygen species; redox state; prostate cancer; androgen

Introduction

Thioredoxin 1 (Trx1) is a redox-sensitive molecule that can be redox-modified during redox signaling or in response to cellular redox changes [1-3]. Trx1 redox modifications involve

Corresponding author: Terry D. Oberley, M.D., Ph.D., Department of Pathology and Laboratory Medicine, University of Wisconsin School of Medicine and Public Health, 7153 WIMR, 1111 Highland Ave, Madison, WI 53705. Phone: (608)265-6068; toberley@wisc.edu.

several steps. Initial oxidation of Trx1 results in the formation of an intramolecular disulfide bond between cysteines 32 and 35 in the active site. Trx1 has three additional cysteines: Cys62, Cys69, and Cys73. Further oxidation of Trx1 leads to the formation of a second intramolecular disulfide bond (S—S) between Cys62 and Cys69, and then to an intermolecular disulfide bond between Cys73 of two different Trx1 molecules, which ultimately leads to the formation of a dimmer [3]. Trx1 in which all cysteine residues are oxidized is biochemically inactive. The redox state of Trx1 can be determined by the redox western blot assay measuring the redox state of two pairs of cysteine residues (Cys32, Cys35 and Cys62, Cys69), with the possible results being all 4 cysteine residues reduced, one pair of cysteine residues oxidized in the active site (Cys32, Cys35) to form a disulfide bond, or oxidation of all 4 cysteine residues to form two pairs of disulfide bonds [4]. Analysis of Trx1 by the redox western blot thus provides two important pieces of information: i) the cellular redox status and ii) the activity status of Trx1.

Although there are many redox couples in cells such as NADH/NAD, glutathione/glutathione disulfide, and cysteine/cystine [5], Trx1 is unique because it has a specific role in modulation of redox signaing [4]. Trx1 also has distinct nuclear and cytoplasmic pools, each performing different functions. In the nucleus, Trx1 has been shown to interact with transcription factors such as p53, nuclear factor kappa B (NFκB) and nuclear factor-like 2 (Nrf2), to regulate their binding to DNA [4,6-8]. In the cytoplasm, Trx1 can regulate apoptotic signal-regulating kinases [4,9]. Trx1 is also known to move from the cytoplasm to the nucleus in response to oxidative stress [4]. Selective oxidation of Trx1 can occur and has been detected in both the nucleus and cytoplasm in response to cellular redox changes or during redox signaling in certain cell types [1,2,10,11]. However, subcellular redox changes of Trx1 in prostate cancer cells have not been reported to date.

Increased Trx1 protein expression has been detected in multiple cancer tissues and cancer cell lines, and an increase in Trx1 expression was associated with higher tumor grade and has been implicated in the resistance of tumor cells to certain chemotherapies and ROS-generating agents including doxorubicin, mitomycin C, etoposide and ultraviolet radiation [10]. It has been suggested that Trx1 functions as a protective cellular antioxidant and its upregulation protects cancer cells from oxidative stress [10]. However, most of these studies mainly focus on Trx1 protein expression levels, with little attention being given to its subcellular redox states, a critical factor in understanding cancer cell biology and the functional implications of the role of Trx1 in cancer.

Prostate cancer tissues are in a state of redox imbalance, and the Trx /thioredoxin reductase (TrxR) system is frequently upregulated in prostate cancers [10,12]. To better understand the significance of Trx1 upregulation in prostate cancer, we utilized human tissue microarrays to determine protein levels and subcellular distribution of Trx1 and tissue culture models representing prostate cancer progression with the newly developed redox western blot technique to analyze redox changes of Trx1 in the nucleus and cytoplasm during prostate cancer progression.

Materials and Methods

Chemicals and antibodies

Methyltrienolone (R1881: a synthetic androgen) was purchased from PerkinElmer (Waltham, MA). Microspin G-25 columns were purchased from GE Healthcare (Little Chalfont, Bucks, UK). Dichlorofluorescein diacetate (H_2DCFDA) and 5-(and-6)-carboxy-2′, 7′-dichlorofluorescein diacetate (CDCFDA) were purchased from Molecular Probes (Eugene, OR). Vectastain® Universal Elite ABC kit was purchased from Vector Laboratories (Burlingame, CA). Immunopure metal-enhanced DAB substrate kit was

purchased from Thermo Fisher Scientific (Rockford, IL). Silencer Select Validated Trx1 siRNA (sequence 5′-3′: UGACUUCACACUCUGAAGCaa) was purchased from Ambion (Austin, TX). This siRNA is commercial and has been experimentally validated by the company to reduce the expression of the target gene by 80%. Anti-Trx1 antibodies were purchased from AbFrontier Co., Ltd. (Geumcheon-gu, Seoul, Korea). IRDye 800CW Goat Anti-Rabbit IgG was purchased from Li-COR Biosciences (Lincoln, NE). Fetal bovine serum (FBS) was purchased from Tissue Culture Biologicals (Los Alamitos, CA). Charcoal/Dextran treated FBS was purchased from Hyclone (Logan, UT). All other chemicals and reagents were purchased from Sigma Chemical Co., unless otherwise specified.

Cell culture and treatment

Benign human prostate epithelial cells (PrEC) were purchased from Lonza Walkersville Inc. (Walkersville, MA). LNCaP (ATCC CRL-1740) and PC3 (ATCC CRL-1435) cell lines were obtained from the American Type Culture Collection (Manassas, VA). Recent cultures of PC3 and LNCaP cells were analyzed using single-locus short tandem repeats (STR) DNA typing by Biosynthesis Inc. (Lewisville, TX) to authenticate cell identity.

No contamination or misidentification was detected (data not shown). C4-2B cells were purchased from ViroMed Laboratories (Minnetonka, MN). PrEC cells were grown in serum-free prostate epithelial growth media (PrEGM) (Lonza/Cambrex). LNCaP, C4-2B and PC3 cells were maintained in RPMI 1640 supplemented with 5% fetal bovine serum and 1% antibiotic-antimycotic (Life Technologies, Inc., Rockville, MD) at 37°C in a humidified atmosphere of 95% air and 5% CO_2, and cells grown less than 30 passages were used. In experiments designed to assess the effects of androgen treatment, cells were seeded in androgen-depleted media containing 5% Charcoal/Dextran treated FBS and 1% antibiotic-antimycotic for 24 h before R1881 treatment. R1881 concentration used in this study was 1 nM, an optimal dose stimulating growth of LNCaP cells. Vehicle was 0.001% ethanol.

Tissue microarray construction and immunohistochemistry

Paraffin-embedded tissue blocks of prostatectomies from 41 patients were obtained from the Department of Pathology and Laboratory Medicine, University of Wisconsin School of Medicine and Public Health. Approval for use of human prostate tissue was obtained from the University of Wisconsin Institutional Review Board. One millimeter tissue cores containing cancerous tissues and/or adjacent benign epithelial tissues were used for construction of tissue microarrays with 3-9 cores from each patient depending on the heterogeneity of each cancer. Five micrometer paraffin sections on glass slides were deparaffinized in a 60°C oven for 1 h and then rinsed in 3 changes of xylene for 10 min each. Slides were blocked for endogenous peroxidases with 0.3% methanol/hydrogen peroxide for 20 min and then rehydrated in 1 min changes each of 100%, 95%, 75%, and 50% ethanol, then double-distilled H_2O. Heat-induced epitope retrieval was performed using a digital decloaking chamber (BioCare Medical, Concord, CA) for 30 seconds at 120°C in Tris urea buffer, pH 9.5. Slides were then blocked in 2.5% normal horse serum for 20 min at room temperature in a humidified chamber followed by incubation with primary antibodies (Trx1 1:400) overnight at 4°C in a humidified chamber. The slides were then rinsed in 3 changes of 0.5 M Tris-buffered saline (TBS) and incubated with the biotinylated universal secondary antibody (Vector Laboratories Inc., Burlingame, CA) for 30 min, followed by Immunopure Metal-enhanced DAB substrate for 3 min. After rinsing in distilled H_2O, slides were counterstained with hematoxylin, dehydrated, and mounted with coverslips followed by microscopic analysis with digital image capture.

Western blot analysis

Cell pellets were lysed with M-PER mammalian protein extraction reagent (Pierce Biotechnology, Rockford, IL), and protein concentrations were determined using the Bradford assay (Bio-Rad, Philadelphia, PA). Equal amounts of proteins were electrophoresed in 8-15% SDS polyacrylamide gels and then transferred onto nitrocellulose membranes. After incubation with primary antibodies overnight at 4°C, immunoreactive proteins were detected with secondary antibodies and visualized on X-ray film.

Subcellular fractionation

Nuclear and cytoplasmic fractions were prepared from cells as previously described [1,2]. Briefly, cells were washed once with ice-cold PBS, and then were collected in 10 mM HEPES (pH 7.8), 10 mM KCl, 2 mM $MgCl_2$, 0.1 mM EDTA, 0.2 mM NaF and 0.2 mM $Na_3VO4{\cdot}6H_2O$ with protease inhibitors and 50 mM IAA. Cell suspensions were then incubated on ice for 5 min, and NP-40 was added to a final concentration of 0.6%. After centrifugation at 12000g for 5 min, nuclei were pelleted, and the supernatants were retained as the cytoplasmic fraction.

Redox western blotting

Analysis of the redox forms of Trx1 was performed as described previously [1,2,13]. The cytoplasmic and nuclear fractions were used to analyze redox forms of Trx1. After derivatization with 50 mM iodoacetic acid (IAA), excess IAA was removed using microspin G-25 columns. Trx1 redox isoforms were separated by native polyacrylamide gels. For cytoplasmic Trx1, HRP-conjugated anti-rabbit secondary antibody was used and bands were visualized on X-ray film. For nuclear Trx1, IRDye 800CW conjugated goat anti-rabbit secondary antibody was used and bands were visualized using Odyssey scanner (LI-COR, Lincoln, NE, U.S.A.).

Trx activity assay

The insulin disulfide reduction assay was used to measure total Trx activity as previously described [14]. Briefly, total cellular proteins were extracted using a buffer containing 20 mM HEPES (pH 7.9), 300 mM NaCl, 100 mM KCl, 10 mM EDTA, 0.1% Nonidet P-40 and protease inhibitors. Equal amounts of protein (90 μg) extracts were incubated at 37°C for 15 min with 1 μL of activation buffer containing 50 mM HEPES (pH 7.6), 1 mM EDTA, 1 mg/ml bovine serum albumin, and 2 mM dithiothreitol in a total volume of 35 uL to reduce Trx. Reaction buffer (20 μL) containing 200 μl of 1 M HEPES (pH 7.6), 40 μl of 0.2 M EDTA, 40 μl of NADPH (40 mg/ml), and 500 μl of insulin (10 mg/ml) was then added to the samples. The reaction was started by the addition of 5 μL bovine Trx reductase or 5 μL water as control. The samples were incubated for 20 min at 37°C. The reaction was terminated by adding 250 μL of stop solution containing 6 M guanidine hydrochloride and 0.4 mg/ml 5, 5′-dithiobis nitrobenzoic acid in 0.2 M Tris-HCl (pH 8.0), and absorption at 412 nm was measured.

Cytotoxicity assay

Cells (4×10^4) in 24-well plates were treated with or without R1881 for 24 h. After replacing with fresh media, different agents were added for an additional 3 days. MTT assay was performed to determine cell viability as described previously [15]. The percentage of viable cells was calculated as the relative ratio of absorption of the experimental group to the control.

Determination of ROS levels

ROS was measured with dichlorofluorescein diacetate (H_2DCFDA) as described previously [16]. Cells were grown in 6 well plates, and incubated with 2 μM H_2DCFDA for 30 min. Oxidation–insensitive dye 5-(and-6)-carboxy-2′,7′-dichlorofluorescein diacetate (CDCFDA) at 2 μM was used to normalize uptake, efflux, and ester cleavage of H_2DCFDA. Fluorescence was measured using a flow cytometer, and data were analyzed using FlowJo 6.1 software (TreeStar, Ashland, OR, USA).

Small interfering RNA (siRNA) transfection

Cells were transfected with 50 nM of Trx1 siRNA or negative control siRNA using nucleofector kits R and V (Lonza, Switzerland) for LNCaP and PC3 respectively. The transfection was performed using electrophoresis with Amaxa Nucleofector (Lonza, Switzerland) according to manufacturer's instructions. Following transfection, cells were seeded into 24-well plates and then fresh media were replaced for 24 h before treatment with different agents.

Statistical analysis

All experiments were performed three times. Statistical significance was examined using Student's *t* test unless specified. The two-sample *t* test was used for two-group comparison. Values were reported as means ± SD. $p<0.05$ was considered significant. The relationship between the intensity of Trx1 staining, primarily in the nucleus, and prostate cancer stages was analyzed using Fisher's Exact Test for count data with simulated *p*-value using R software (Institute for Statistics and Mathematics, WU Wien). $p<0.05$ was considered significant.

Results

Elevated nuclear Trx1 expression in high-grade human prostate cancer cells

Immunohistochemical staining was performed in human prostate tissue microarrays. The benign prostatic epithelium (Fig. 1A) and high-grade prostatic intraepithelial neoplasia (HG-PIN) (Fig. 1B) examined were located adjacent to adenocarcinoma (Fig 1F). Immunohistochemistry demonstrated a moderate degree of finely granular staining for Trx1 in the cytoplasm and nuclei and focally strong nuclear staining for Trx1 in benign epithelium, HG-PIN and low-grade prostatic adenocarcinoma cells (Fig. 1A, 1B, and 1C). High-grade prostatic adenocarcinoma and metastatic prostatic adenocarcinoma cells showed diffuse strong nuclear staining for Trx1 (Fig. 1D and 1E). No significant staining was detected in control samples without primary antibody added. Semiquantitative analysis of immunohistochemical staining in human prostate tissue microarrays showed a strong correlation between the intensity of Trx1 staining, primarily in the nucleus, and prostate cancer progression (Table 1).

Alteration of nuclear Trx1 during prostate cancer progression

To simulate prostate cancer progression, we analyzed a tissue culture model in which normal prostate epithelial cells were compared to prostate cancer cell lines of increasing degree of aggressiveness. We used PrEC cells representing normal prostate epithelial cells, less aggressive LNCaP cells representing low grade prostate cancer, intermediate aggressive C4-2B cells simulating intermediate grade prostate cancer, and more aggressive PC3 cells as an example of high grade prostate cancer. The tissue culture model of prostate cancer progression was validated in our experiments (Fig S1). LNCaP and C4-2B cells were androgen receptor (AR) positive (Fig. S1A), and showed androgen-inducible prostate specific antigen (PSA) expression (Fig. S1A), growth and invasion (Fig. S1B and S1C).

C4-2B cells were less androgen-dependent, had higher growth and invasion potential, and produced a substantially higher amount of basal steady-state concentrations of PSA in androgen-depleted media (Fig. S1). PC3 cells were AR-negative and showed androgen-independent growth and invasion (Fig. S1), thus serving as a model of more aggressive androgen-independent prostate cancer. PrEC, benign prostate epithelial cells, were used as a normal control for our studies (Fig. S1). Predominant evidence is that PrEC cells are derived from the basal cells of prostate glands without the expression of AR [17], which was also demonstrated in our studies (Fig. S1).

There was a significant increase in nuclear Trx1 levels with the development and progression of cancer (PC3>C4-2B/LNCaP> PrEC) (Fig. 2A). In the cytoplasm, Trx1 was also significantly increased in PC3 cells in comparison to the other types of cells (Fig. 2A). The level of increase was more pronounced in the nucleus than in the cytoplasm, with more than four times increase in the nucleus and less than two times increase in the cytoplasm (Fig. 2A). We also examined subcellular Trx1 expression in response to androgens, in various cell types in tissue culture studies. Treatment with R1881, a synthetic androgen, increased nuclear Trx1 protein levels without significant effect on cytoplasmic Trx1 protein levels in LNCaP and C4-2B cell lines (Fig. 2B). Induction was detected at 30 min following R1881 treatment and reached peak values at 24 h. Levels were maintained at a steady state afterwards (Fig. 2B). No such changes were detected in either PC3 or PrEC cells (Fig. 2B).

Analysis of redox states of nuclear and cytoplasmic Trx1 in response to R1881 during prostate cancer progression

Redox western analysis was used to determine the relative amounts of reduced and oxidized Trx1 in prostate cancer cell lines following R1881 treatment. After treatment with IAA, Trx1 showed 3 bands: fully reduced, one-disulfide and two-disulfide bands. The redox state of nuclear Trx1 was more reduced in PrEC cells than in the three prostate cancer cell lines (Fig. 3B), but in none of the cell types did androgen affect the relative ratio of reduced to oxidized Trx1 in the nuclei (Fig. 3A). In untreated controls, Trx1 was predominantly in the reduced state in the cytosolic fractions (Fig. 3C, 0 h). However, in response to R1881, a transient increase in cytoplasmic Trx1 oxidation was detected in AR positive, androgen-responsive LNCaP and C4-2B cells, but not in the AR negative, androgen-nonresponsive PrEC and PC3 cells (Fig. 3C). In untreated cells, the basal levels of redox states of cytoplasmic Trx1 were not changed during the time points examined (data not shown). There was a clear difference in the pattern of cytoplasmic Trx1 oxidation in comparison of LNCaP to its more aggressive C4-2B derivative. The transient increase in Trx1 oxidation lasted for a shorter time in LNCaP cells than in C4-2B cells. In addition, in untreated controls, PC3 cells had significantly higher levels of the oxidized forms of Trx1 in the cytoplasm than LNCaP and C4-2B cells (Fig. 3C). PrEC cells also displayed a higher oxidation state of cytoplamic Trx1 than LNCaP and C4-2B cells (Fig. 3C), but the cytoplasmic Trx1 was more reduced in PrEC cells than PC3 cells (Fig. 3C).

Decreased Trx activity with the progression of prostate cancer

Trx activity assay demonstrated a slight increase in Trx activity in LNCaP and C4-2B cells after treatment with R1881 in comparison to untreated controls (Fig. 4). Trx activities were lower in all 3 prostate cancer cell lines than PrEC cells, with the lowest observed in the more aggressive PC3 cells.

Increased sensitivity to pro-oxidant-induced cell death with the progression of prostate cancer

Prostate cancer cells were treated with various concentrations of BCNU or L-buthionine sulfoximine (BSO), two low molecular weight compounds that shift intracellular redox state

towards oxidation [5]. Cell viability was assessed using MTT assay. Dose-dependent cytotoxicity was observed in all the cell lines tested, but the dose with the least toxic effect was chosen for comparison of cell viability in the three cancer cell lines. As shown in Fig. 5, the viability of more aggressive PC3 cells was significantly lower than that of LNCaP and C4-2B cells treated with the same concentration of either 50 μM BCNU or 2 mM BSO, suggesting a more oxidizing intracellular milieu in PC3 cells. Androgen treatment increased the cellular resistance to these compounds in LNCaP and C4-2B cells (Fig. 5A and 5B), but not in PC3 cells. The increase in resistance was higher in LNCaP cells than its less androgen responsive C4-2B counterpart (Fig 5A and 5B).

Alteration of pro-oxidant-induced cytotoxicity by Trx1 knockdown in prostate cancer cells

We next determined the role of Trx1 in BCNU- or BSO-induced cytotoxicity using siRNA knockdown technology to reduce mRNA of Trx1. In this study, we use commercial Silencer Select Validated Trx1 siRNA, which has been experimentally validated by the company to reduce the expression of the target gene by 80%. The control siRNA transfection did not affect Trx1 protein expression, ROS levels or sensitivity to BSO- or BCNU- induced cytotoxicity (data not shown). In contrast, Trx1 siRNA transfection reduced Trx1 protein levels (Fig. 6A), elevated ROS levels (Fig. 6B), and increased sensitivity to BSO- or BCNU-induced cytotoxicity in all cancer cell lines (Fig. 6C). Redox insensitive CDCF fluorescence was not changed in LNCaP cells with Trx1 siRNA transfection (data not shown). The enhanced sensitivity to BCNU- or BSO-induced cytotoxicity was higher in less aggressive LNCaP cells than in PC3 cells. In addition, androgen treatment resulted in a significant increase in Trx1 levels (Fig. 6A) and a corresponding decrease in ROS levels (Fig. 6B) in LNCaP cells, which was correlated to the androgen-induced resistance to BCNU or BSO. Androgen-induced resistance to the cytotoxicity of BCNU or BSO in LNCaP cells was significantly diminished by Trx1 siRNA transfection (Fig. 6C), suggesting the possible role of Trx1 in androgen-induced resistance to pro-oxidant treatment and in maintaining redox balance within these cells.

Discussion

In this study, we are the first group to report the use of Trx1 redox states to study subcellular redox imbalance in prostate cancer. The results demonstrated herein would enhance the understanding of prostate cancer development and progression. Our study, for the first time, demonstrated increased levels of nuclear Trx1 from low grade to high grade human prostate cancers (Fig. 1 and Table 1) and constitutively high levels of total and oxidized forms of Trx1 in the nucleus in prostate cancer cell lines from low to high aggressiveness compared to their benign counterparts (Fig 2 and 3). These results suggest nuclear redox imbalance may occur in the early stage of cancer development and progressively shift to a more oxidative state with cancer progression, which may be a contributing factor to DNA damage and subsequent gene mutation, genomic instability and other events that lead to cancer development and progression. Additionally, our study demonstrated that Trx1 was a highly redox-sensitive biomarker and its redox states in the nucleus and cytoplasm could be differentially assessed by redox western blot analyses (Fig. 3). Our study also demonstrated that total Trx activity was correlated with Trx1 redox states, active in the reduced state and inactive in the oxidative state (Fig. 3 and 4). Thus, although Trx1 protein levels were greatly increased in highly aggressive PC3 cells, there was a significant decrease in total Trx activity and a high level of Trx1 oxidation (Fig. 2 and 3), suggesting oxidation is an important factor in regulating Trx activity. Importantly, the study showed that a growth-stimulating dose of androgen upregulated Trx1 and decreased sensitivity to the cytotoxicity of pro-oxidant compounds (Fig. 5), while downregulation of Trx1 by silencing RNA increased the sensitivity to the cytotoxicity of these compounds (Fig. 6), implicating the

involvement of cell redox state in regulation of prostate cancer cell growth and protection of Trx1 against oxidative stress and cell death.

It is known that Trx1 can interact with and regulate several important tumor suppressing or promoting proteins such as p53, NFκ-B and Nrf-2 in the nucleus [4,6-8]. Oxidation of Trx1 in the nucleus may imply possible redox modifications of these proteins, potentially contributing to prostate cancer development and progression. Reduced Trx1 can also induce manganese superoxide dismutase (MnSOD) mRNA levels, possibly affecting mitochondrial function [18]. Studies by Zhao et al. showed that suppression of MnSOD activity in the mitochondria by direct interaction of p53 with MnSOD protein was an early event of tumor promoter-induced skin carcinogenesis, possibly contributing to increased oxidative stress and subsequent enhanced cell proliferation and apoptosis during the promotion phase of skin tumorigenesis [19,20]. Administration of MnSOD mimics before cell proliferation resulted in reduction of the incidence and multiplicity of skin tumors in the same skin carcinogenesis mouse model [20]. Therefore, the oxidation of Trx1 observed with the progression of prostate cancer could also result in the modulation of MnSOD, affecting p53 activity and thus possibly contributing to increased oxidative stress and the development of prostate cancer.

In the cytoplasm, ROS has been shown to activate the phosphoinositide 3-kinase (PI3K)/Akt, a pathway that is known to contribute to prostate cancer progression by increasing cell survival and growth while inhibiting apoptosis [12]. The increased cytoplasmic Trx1 oxidation during progression of prostate cancer (Fig. 3C) demonstrated in this study may be a direct indicator of increased activation of such pathways. Cytoplasmic Trx1 oxidation in PrEC cells may due to the activation of growth factor signaling since PrEC cells were cultured in growth factor-enriched media and cytoplasmic Trx1 has been shown to be oxidized during growth factor signaling [1].

Previous studies showed that growth-stimulating concentration of androgens lowered ROS levels in LNCaP cells [21], which was also demonstrated in our studies (Fig. 6B). However, subcellular redox changes of Trx1 were unknown at the time of this earlier study. Our study first documented constitutively increased Trx1 protein levels in the nucleus (Fig. 2) and a transient cytoplasmic oxidation of Trx1 (Fig. 3C) following androgen treatment in androgen responsive LNCaP and C4-2B cells. This result is similar to a previous study showing selective cytoplasmic Trx1 oxidation during epidermal growth factor signaling,[1] suggesting a possible involvement of redox signaling regulated by androgens. In comparison to LNCaP cells, cytoplasmic Trx1 oxidation was prolonged in more aggressive C4-2B cells following androgen treatment and constitutively remained at higher levels in PC3 cells (Fig. 3C), suggesting the presence of a redox regulatory mechanism in response to androgens in androgen-responsive cells, and this regulation may be gradually lost during prostate cancer progression. Trx1 may be a part of this regulatory system since the sensitivity of cells to pro-oxidants treatment was increased in PC3 cells with higher oxidation of Trx1 and less total activity of Trx (Fig. 4). Increased Trx1 expression induced by androgens reduced ROS levels and increased the resistance of cancer cells to these agents (Fig. 5 and 6), while decreased Trx1 expression by silencing RNA showed the opposite results (Fig. 6). This is consistent with the theory that ROS have interacted with Trx1 following androgen exposure. This result also provides additional evidence that Trx1 can serve as important subcellular biomarker of redox signaling or subcellular redox changes.

Analysis of Trx1 redox states could significantly enhance our understanding of the role of Trx1 in cancer. Increased Trx expression has been linked to higher tumor grade and implicated in the resistance of tumor cells to certain chemotherapies [10], and the upregulation of Trx has been suggested to function as a cellular antioxidant to protect cancer

cells from oxidative stress [10]. However, oxidation of Trx1 despite the significant increase in Trx1 protein levels (Fig. 1,2 and 3) in prostate cancer in our studies clearly demonstrated that prostate cancer cells failed to establish redox balance even with increased Trx1 levels, and Trx1 in prostate cancer may have partially lost its antioxidant capacity. The specific accumulation of Trx1 proteins in the nucleus (Fig. 1 and 2) may also represent an adaptation of cancer cells in combating chronic exposure to oxidative stress since it is known that Trx1 translocates into the nucleus in response to oxidative stress [4].

Previous studies showed no significant association between the extent of increase in Trx expression and response to docetaxel monotherapy in breast cancers [22]. This can be explained by our results showing that the response of cancer cells to agents that can cause redox imbalance depends not only on Trx1 expression levels, but the effects of redox states on Trx activity. Increased cell killing by BCNU and BSO, two agents that cause redox imbalance, was observed in PC3 cells with higher oxidation states of Trx1 and lower Trx activity despite the higher protein expression levels (Fig. 5). Elevated Trx1 expression induced by androgens increased the resistance of prostate cancer cells to the cytotoxicity of pro-oxidant compounds (Fig. 5), while reduced Trx1 expression by silencing RNA decreased the resistance (Fig. 6), which had more effect on LNCaP cells with less Trx1 oxidation and higher Trx activity than PC3 cells (Fig. 6). These results suggest that not only the protein level, but also the redox states affect Trx activity and the response of prostate cancer cells to these agents. Downregulation of Trx1 by silencing RNA slightly increased ROS levels in all cancer cell lines, but had the most significant effect on LNCaP cells, suggesting a role of Trx1 in controlling redox imbalance in prostate cancer.

Recent studies on targeting thioredoxin systems in cancers have shown promising but some conflicting results. For example, stable overexpression of Trx1 by cDNA transfection failed to increase the resistance of ovarian and colon cancer cell lines to chemotherapeutic agents [23], although Trx1 antisense expression reversed the resistance of bladder cancer cell lines [24]. Low doses of the Trx inhibitor, PMX464, were not effective in colorectal cancer cell lines under normoxic conditions [25]. Overexpression of thioredoxin interacting protein (TXNIP) in melanoma cells increased transendothelial migration [26]. Another study on microvascular endothelial cell migration showed that silencing Trx abrogated all angiogen-induced migration, while silencing TXNIP strongly induced migration [27]. Although future studies are needed to define the molecular mechanism underlying these conflicting results, it is possible that differences in oxidation states and different functions of Trx1 in each cancer cell type may be determinant factors for those different responses. Therefore, Trx1 redox states should be analyzed as well as protein expression levels in defining subcellular redox states and in analyzing the effects of Trx modulation in cancers and possible therapeutic effects of Trx inhibitors.

In this study, we also analyzed the correlation of Trx activity assay with Trx1 redox states (Fig. 3). Potential problems with the use of the Trx activity assay include the following: i) the assay includes a step of DTT reduction and use of TrxR, which will result in reactivation of reversibly oxidized Trx; ii) the substrate specificity is unknown in using recombinant or other non-human TrxR, and the Trx activity assay could differentiate neither different isoforms of Trx, such as Trx1 and Trx2, nor the contribution of Trx interacting proteins such as TrxR and TXINP. However, DTT will not activate irreversibly oxidized Trx [28], and our results demonstrated a loss of Trx activity even with increased Trx1 protein levels in cancer cells. Trx activity correlated well with ROS levels as determined by DCF florescence. Reduced Trx activity correlated with higher levels of ROS in PC3 cells, while increased Trx activity by androgen treatment was associated with lower levels of ROS in LNCaP cells. Although new studies would be necessary to delineate the activities or effects of Trx1, Trx2, TrxR1, TrxR2 and TXINP, in order to fully understand the significance of the decrease in

total Trx activities, the results in this study indicate the importance of the redox state of Trx1 and the value of the redox western blot analysis. Redox western blot studies can differentially analyze different isoforms of Trx and also delineate total amount of proteins as well as the different redox states and the activity status of Trx (from fully oxidized to fully reduced Trx) without introducing exogenous TrxR [10].

Oxidation of Trx1 may also result from decreased TrxR1 or increased TXINP. It has been shown that TXINP mRNA was decreased, while TrxR1 level was increased in PC3 cells in comparison to LNCaP cells, suggesting a complementary regulatory system for Trx1 oxidation. Although future studies will be very necessary to delineate mechanisms underlying Trx1 oxidation and identify potential drug targets for prostate cancer, the oxidation of Trx1 and accumulation of Trx1 in the nucleus clearly demonstrated increased subcellular redox imbalance with the progression of prostate cancer.

In summary, this study is the first to identify constitutive nuclear and transiently increased cytoplasmic Trx1 oxidation by androgen, but decreased Trx activities with the progression of prostate cancer, despite high levels of Trx1 protein expression in cancer cells. The sensitivity of cancer cells to redox-modulating agents was predicted not only by Trx1 protein levels, but also its redox states and Trx activity. These findings significantly improve our understanding of the role of cell redox regulation in prostate cancer development and progression, expand our knowledge of the role of Trx1 in cancer, and provide important information on developing potential new strategies for prostate cancer treatment. The results suggest that Trx1 redox status may serve as a biomarker for monitoring subcellular redox imbalance in prostate cancer.

Supplementary Material

Refer to Web version on PubMed Central for supplementary material.

Acknowledgments

The authors thank the laboratory of Dr. Dean P Jones for technical advice, Joan Sempf and Jamie Swanlund for technical assistance, and Dr. Lukasana Chaiswing for sending the cells to Biosynthesis Inc (Lewisville, TX) to authenticate cell identity. The contents do not represent the views of the department of Veterans Affairs of the United States Government.

Grant Support: This work was supported by funds from the University of Wisconsin, Department of Pathology Research and Development Committee, grant P30 CA014520 from the National Cancer Institute, NIH grants RO1 CA073599, RO1 CA094853, RO1 AG012350 and RO1 CA115801, and supported with resources and facilities at the William S. Middleton Memorial Veterans Hospital, Madison, WI.

References

1. Halvey PJ, Watson WH, Hansen JM, Go YM, Samali A, Jones DP. Compartmental oxidation of thiol-disulphide redox couples during epidermal growth factor signalling. Biochem J. 2005; 386:215–219. [PubMed: 15647005]
2. Go YM, Ziegler TR, Johnson JM, Gu L, Hansen JM, Jones DP. Selective protection of nuclear thioredoxin-1 and glutathione redox systems against oxidation during glucose and glutamine deficiency in human colonic epithelial cells. Free Radic Biol Med. 2007; 42:363–370. [PubMed: 17210449]
3. Sun Y, Rigas B. The thioredoxin system mediates redox-induced cell death in human colon cancer cells: implications for the mechanism of action of anticancer agents. Cancer Res. 2008; 68:8269–8277. [PubMed: 18922898]
4. Hansen JM, Go YM, Jones DP. Nuclear and mitochondrial compartmentation of oxidative stress and redox signaling. Annu Rev Pharmacol Toxicol. 2006; 46:215–234. [PubMed: 16402904]

5. Schafer FQ, Buettner GR. Redox environment of the cell as viewed through the redox state of the glutathione disulfide/glutathione couple. Free Radic Biol Med. 2001; 30:1191–1212. [PubMed: 11368918]
6. Hayashi T, Ueno Y, Okamoto T. Oxidoreductive regulation of nuclear factor kappa B. Involvement of a cellular reducing catalyst thioredoxin. J Biol Chem. 1993; 268:11380–11388. [PubMed: 8496188]
7. Ueno M, Masutani H, Arai RJ, Yamauchi A, Hirota K, Sakai T, Inamoto T, Yamaoka Y, Yodoi J, Nikaido T. Thioredoxin-dependent redox regulation of p53-mediated p21 activation. J Biol Chem. 1999; 274:35809–35815. [PubMed: 10585464]
8. Hansen JM, Watson WH, Jones DP. Compartmentation of Nrf-2 redox control: regulation of cytoplasmic activation by glutathione and DNA binding by thioredoxin-1. Toxicol Sci. 2004; 82:308–317. [PubMed: 15282410]
9. Saitoh M, Nishitoh H, Fujii M, Takeda K, Tobiume K, Sawada Y, Kawabata M, Miyazono K, Ichijo H. Mammalian thioredoxin is a direct inhibitor of apoptosis signal-regulating kinase (ASK) 1. Embo J. 1998; 17:2596–2606. [PubMed: 9564042]
10. Mukherjee A, Martin SG. The thioredoxin system: a key target in tumour and endothelial cells. Br J Radiol. 2008; 81(Spec No 1):S57–68. [PubMed: 18819999]
11. Go YM, Jones DP. Redox control systems in the nucleus: mechanisms and functions. Antioxid Redox Signal. 13:489–509. [PubMed: 20210649]
12. Kumar B, Koul S, Khandrika L, Meacham RB, Koul HK. Oxidative stress is inherent in prostate cancer cells and is required for aggressive phenotype. Cancer Res. 2008; 68:1777–1785. [PubMed: 18339858]
13. Watson WH, Pohl J, Montfort WR, Stuchlik O, Reed MS, Powis G, Jones DP. Redox potential of human thioredoxin 1 and identification of a second dithiol/disulfide motif. J Biol Chem. 2003; 278:33408–33415. [PubMed: 12816947]
14. Wang Y, De Keulenaer GW, Lee RT. Vitamin D(3)-up-regulated protein-1 is a stress-responsive gene that regulates cardiomyocyte viability through interaction with thioredoxin. J Biol Chem. 2002; 277:26496–26500. [PubMed: 12011048]
15. Zhao R, Xiang N, Domann FE, Zhong W. Expression of p53 enhances selenite-induced superoxide production and apoptosis in human prostate cancer cells. Cancer Res. 2006; 66:2296–2304. [PubMed: 16489034]
16. Chaiswing L, Bourdeau-Heller JM, Zhong W, Oberley TD. Characterization of redox state of two human prostate carcinoma cell lines with different degrees of aggressiveness. Free Radic Biol Med. 2007; 43:202–215. [PubMed: 17603930]
17. Sobel RE, Wang Y, Sadar MD. Molecular analysis and characterization of PrEC, commercially available prostate epithelial cells. In Vitro Cell Dev Biol Anim. 2006; 42:33–39. [PubMed: 16618209]
18. Das KC, Lewis-Molock Y, White CW. Elevation of manganese superoxide dismutase gene expression by thioredoxin. Am J Respir Cell Mol Biol. 1997; 17:713–726. [PubMed: 9409558]
19. Zhao Y, Chaiswing L, Velez JM, Batinic-Haberle I, Colburn NH, Oberley TD, St Clair DK. p53 translocation to mitochondria precedes its nuclear translocation and targets mitochondrial oxidative defense protein-manganese superoxide dismutase. Cancer Res. 2005; 65:3745–3750. [PubMed: 15867370]
20. Zhao Y, Chaiswing L, Oberley TD, Batinic-Haberle I, St Clair W, Epstein CJ, St Clair D. A mechanism-based antioxidant approach for the reduction of skin carcinogenesis. Cancer Res. 2005; 65:1401–1405. [PubMed: 15735027]
21. Ripple MO, Henry WF, Rago RP, Wilding G. Prooxidant-antioxidant shift induced by androgen treatment of human prostate carcinoma cells. J Natl Cancer Inst. 1997; 89:40–48. [PubMed: 8978405]
22. Kim SJ, Miyoshi Y, Taguchi T, Tamaki Y, Nakamura H, Yodoi J, Kato K, Noguchi S. High thioredoxin expression is associated with resistance to docetaxel in primary breast cancer. Clin Cancer Res. 2005; 11:8425–8430. [PubMed: 16322305]

23. Yamada M, Tomida A, Yoshikawa H, Taketani Y, Tsuruo T. Overexpression of thioredoxin does not confer resistance to cisplatin in transfected human ovarian and colon cancer cell lines. Cancer Chemother Pharmacol. 1997; 40:31–37. [PubMed: 9137526]

24. Yokomizo A, Ono M, Nanri H, Makino Y, Ohga T, Wada M, Okamoto T, Yodoi J, Kuwano M, Kohno K. Cellular levels of thioredoxin associated with drug sensitivity to cisplatin, mitomycin C, doxorubicin, and etoposide. Cancer Res. 1995; 55:4293–4296. [PubMed: 7671238]

25. Mukherjee A, Westwell AD, Bradshaw TD, Stevens MF, Carmichael J, Martin SG. Cytotoxic and antiangiogenic activity of AW464 (NSC 706704), a novel thioredoxin inhibitor: an in vitro study. Br J Cancer. 2005; 92:350–358. [PubMed: 15655539]

26. Le Jan S, Le Meur N, Cazes A, Philippe J, Le Cunff M, Leger J, Corvol P, Germain S. Characterization of the expression of the hypoxia-induced genes neuritin, TXNIP and IGFBP3 in cancer. FEBS Lett. 2006; 580:3395–3400. [PubMed: 16723126]

27. Ng MK, Wu J, Chang E, Wang BY, Katzenberg-Clark R, Ishii-Watabe A, Cooke JP. A central role for nicotinic cholinergic regulation of growth factor-induced endothelial cell migration. Arterioscler Thromb Vasc Biol. 2007; 27:106–112. [PubMed: 17082486]

28. Hashemy SI, Holmgren A. Regulation of the catalytic activity and structure of human thioredoxin 1 via oxidation and S-nitrosylation of cysteine residues. J Biol Chem. 2008; 283:21890–21898. [PubMed: 18544525]

Abbreviations

AR	androgen receptor
BCNU	carmustine
BSO	L-buthionine sulfoximine
CDCFDA	5-(and-6)-carboxy-2′,7′-dichlorofluorescein diacetate
H_2DCFDA	dichlorofluorescein diacetate
IAA	iodoacetic acid
MnSOD	Manganese superoxide dismutase
NFκB	nuclear factor kappa B
Nrf2	nuclear factor-like 2
PrEC	benign prostate epithelial cells
PSA	prostate specific antigen
ROS	reactive oxygen species
TTBS	Tween 20 Tris-buffered saline
Trx	thioredoxin
TrxR	thioredoxin reductase
TXNIP	thioredoxin interacting protein

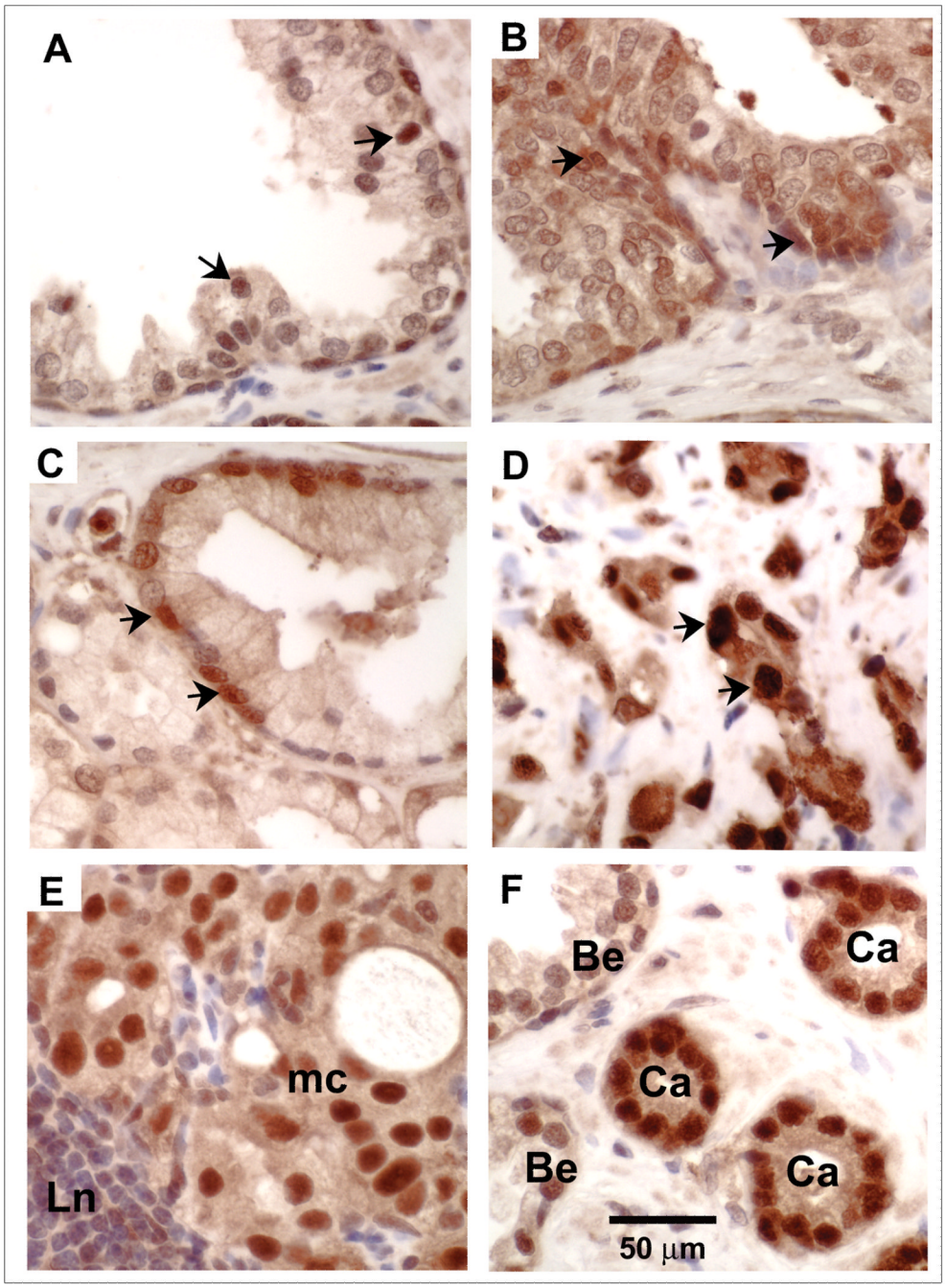

Figure 1. Immunohistochemical detection of Trx-1 protein levels in human prostatic tissues

A-D, Representative micrographs of benign prostatic epithelium (**A**), HG-PIN (**B**), low-grade prostatic adenocarcinoma (Gleason pattern 2) (**C**), High-grade prostatic adenocarcinoma (Gleason pattern 4) (**D**), metastatic prostatic adenocarcinoma (mc) in a lymph node (Ln) (**E**), prostatic adenocarcinoma (Ca) and benign epithelium (Be) (**F**). Arrows, strong nuclear staining. (magnification: 400×). Sections of human prostate tissue microarrays were examined immunohistochemically using an anti-Trx1 antibody.

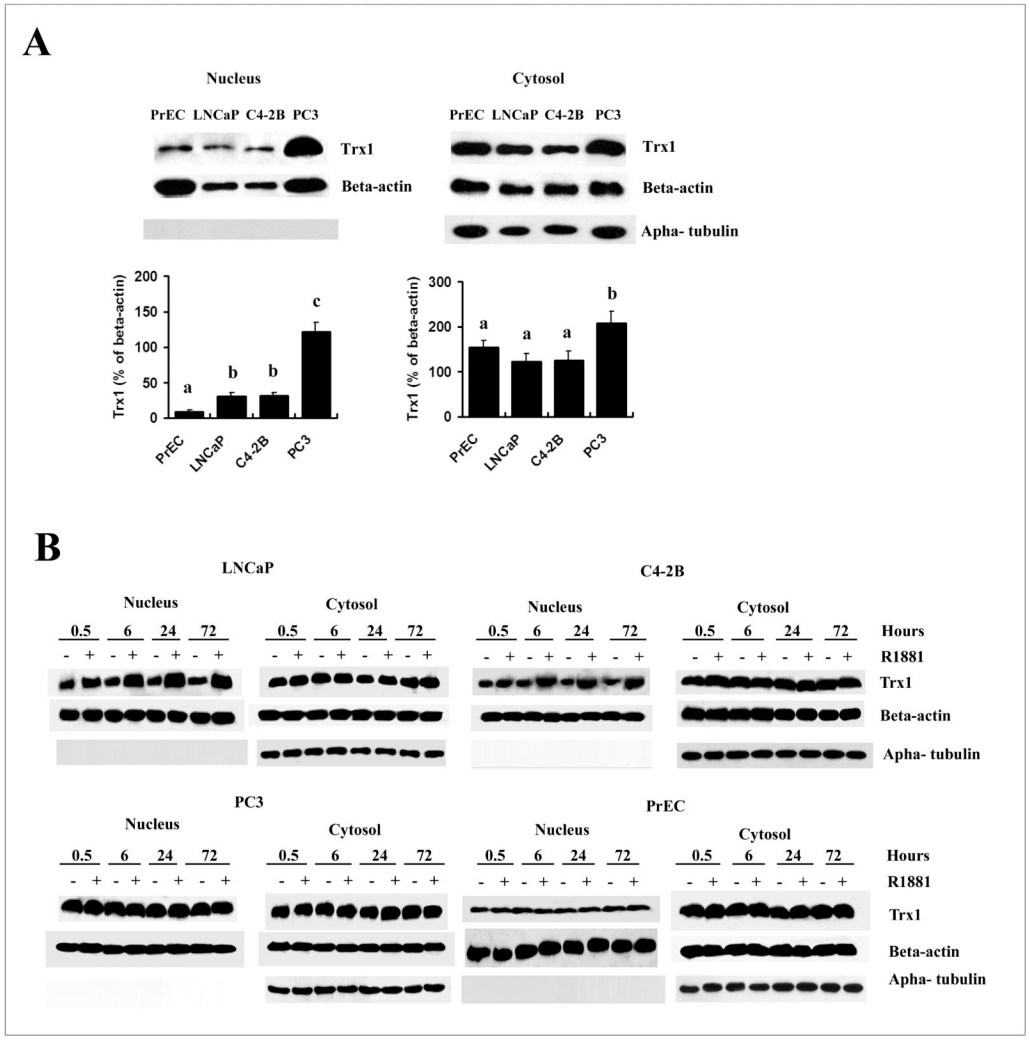

Figure 2. Western blot analysis of effects of R1881 on nuclear and cytoplasmic Trx1 protein expression levels in PrEC and prostate cancer cells

A, Comparison of Trx1 expression level in the nucleus and cytoplasm with the progression of prostate cancer. Basal level of Trx1 expression in the nucleus and cytoplasm of different cell lines without treatment with R1881 were loaded in the same SDS gel and compared. Data are presented as means ± SD. Means with different letters above bars indicate significant differences ($P < 0.05$) in each panel. **B,** Time course of Trx1 protein expression levels in the nucleus or cytoplasm in LNCaP, C4-2B, PC3, or PrEC cells following R1881 treatment at various time points. Cells were treated with ethanol (0.001% EtOH) vehicle control or 1 nM R1881 and nuclear and cytoplasmic proteins were processed as outlined in Materials and Methods. Purity of the nuclear fractions was assured by immunoblotting with an anti-alpha-tubulin antibody. Protein loading: 50 μg for nuclear proteins and 30 μg for cytoplasmic proteins.

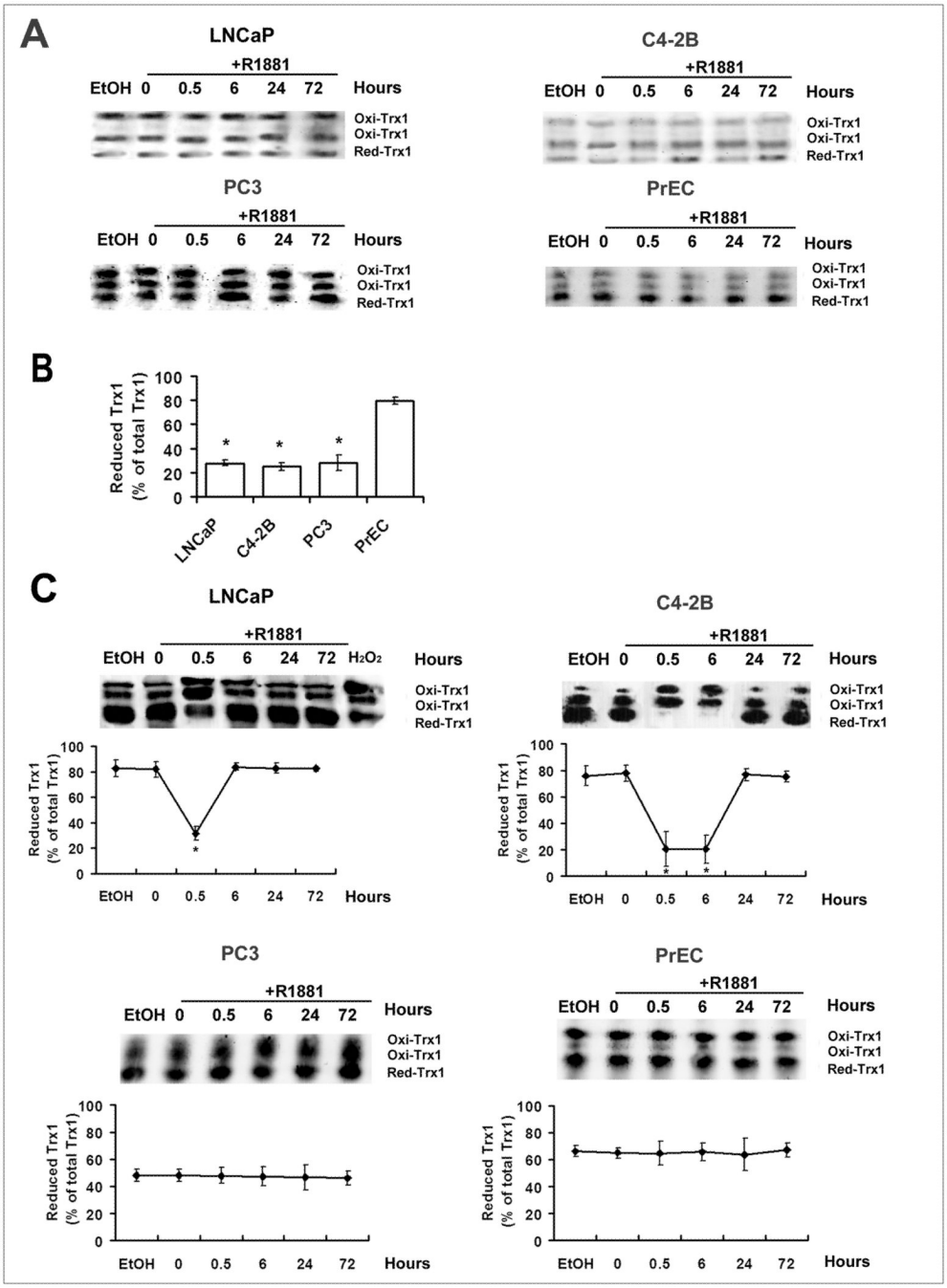

Figure 3. Redox western blot analysis of effects of R1881 on redox states of nuclear and cytoplasmic Trx1 in PrEC and prostate cancer cells

A and **C,** Time course of Trx1 reduction/oxidation in the nucleus (**A**), and cytoplasm (**C**) of PrEC, LNCaP, C4-2B or PC3 cells following R1881 treatment at various time points. **B,** Comparison of nuclear Trx1 redox states in prostate cancer cells with PrEC cells. Cells were treated with ethanol (0.001% EtOH) vehicle control or 1 nM R1881. Nuclear or cytoplasmic proteins were processed as outlined in Materials and Methods. Redox forms of Trx1 are indicated as follows: *red*, reduced form; *oxi*, oxidized form (disulfide in active site); the top *oxi* band representing the most oxidized form (disulfides in active site and outside active site). H_2O_2 (0.1 mM, 10 min) treated cellular extracts were used as a positive control. The

percentage of Trx1 in the reduced form was calculated by the formula % Reduced= reduced Trx1/total Trx1 (total of 3 bands). Data are presented as means ± SD. *, $p<0.05$ compared with control.

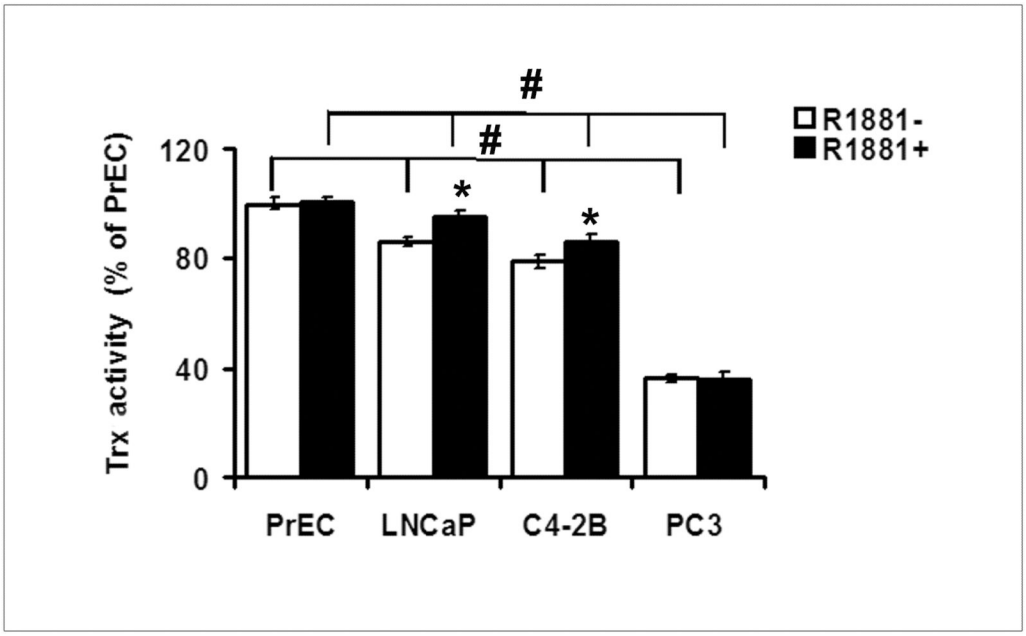

Figure 4. Total Trx activity in PrEC and prostate cancer cells

Cells were treated with ethanol (0.001% EtOH) vehicle control or 1.0 nM R1881 for 24 h, Trx activity was measured using the insulin reduction assay as described in Materials and Methods. Data are presented as means ± SD. *, $p<0.05$ compared with the corresponding control without R1881 treatment. #, $p<0.05$ compared between cell types.

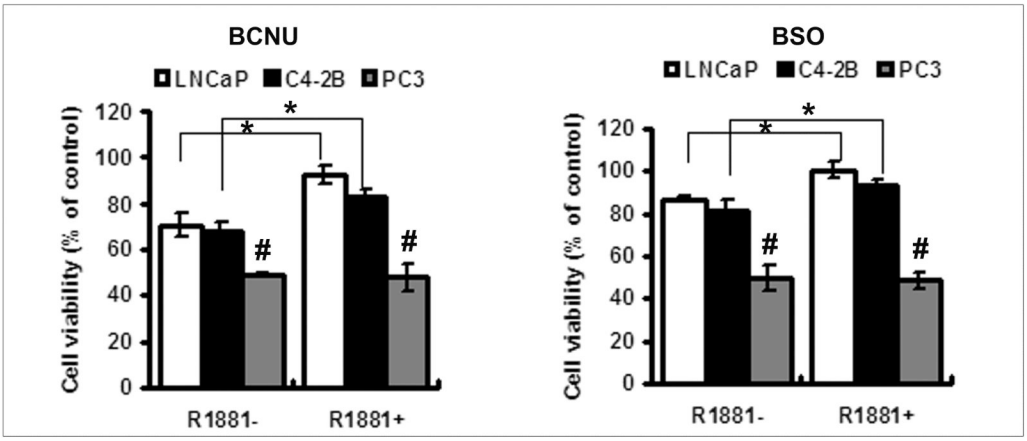

Figure 5. Effects of R1881 on cancer cell viability treated with BCNU or BSO

The effects of R1881 on cell viability of prostate cancer cells treated with 50 μM BCNU (**A**) or 2 mM BSO (**B**). After pretreatment with or without 1.0 nM R1881 for 1 day, cells were then treated with 50 μM BCNU (**A**) or 2 mM BSO (**B**) for 3 days, and cell viabilities were measured as described in Materials and Methods. Data are presented as means ± SD. *, $p<0.05$ compared with control without R1881 treatment. #, $p<0.05$ compared with LNCaP or C4-2 cells with the corresponding treatment.

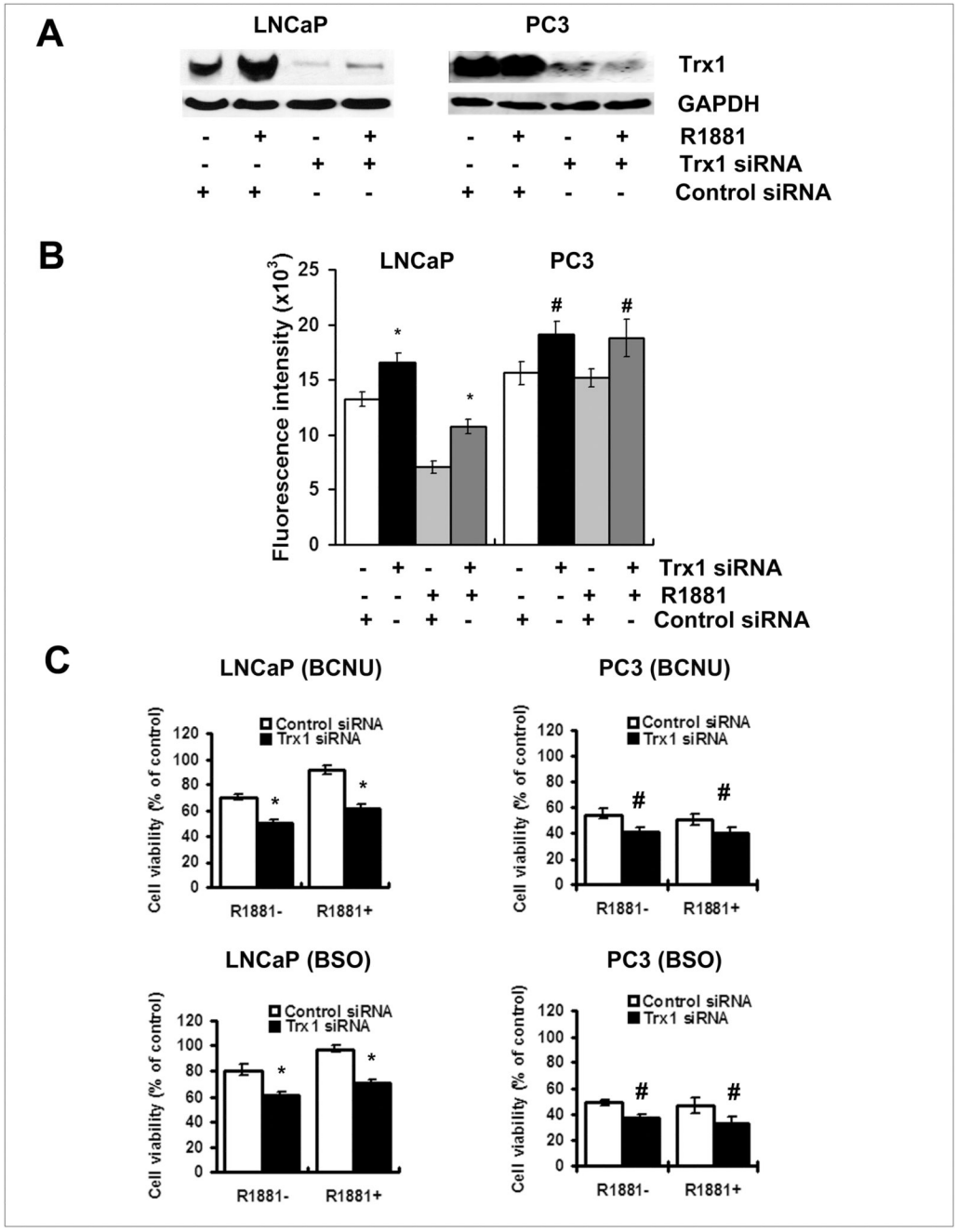

Figure 6. Down-regulation of Trx1 by RNA interference increased ROS levels and sensitivity to BCNU and BSO in prostate cancer cells

A, Western blot analysis showing suppressive effects of Trx1 siRNA transfection on expression of Trx1 in cells with and without 1.0 nM R1881 treatment. **B,** Increased levels of ROS with Trx1 siRNA transfection. Cells were transfected with the control siRNA or Trx1 siRNA in the absence or presence of R1881. **C.** MTT assay of cellular response to 50 μM BCNU or 2 mM BSO following down-regulation of Trx1 by siRNA transfection. After transfection with 50 nmol/L of the control or Trx1 siRNA, cells were cultured for 24 h and then, treated with or without 1.0 nM R1881 for 1 day, Western blot analysis and ROS measurements were then performed. For cell viability assay, cells were treated with 50 μM

BCNU or 2 mM BSO for an additional 3 days. C4-2B had similar results to LNCaP cells (data not shown). Data are presented as means ± SD. *, $p<0.05$ compared with the corresponding control. #, $p<0.1$ compared with the corresponding control.

Free Radic Biol Med. Author manuscript; available in PMC 2011 December 15.

Table 1

Levels of immunoreactive Trx1 protein in human prostate tissues[a]

Pathology	Number of specimens	Negative (−)	Weak (+)	Moderate (++)	Strong (+++)
Benign epithelium	48	0	27 (56%)	16 (33%)	5 (10%)
High grade prostatic intraepithelial neoplasia	70	0	33 (47%)	34 (49%)	3 (4%)
Gleason pattern 2	2	0	1 (50%)	1 (50%)	0
Gleason pattern 3	120	0	2 (2%)	97 (81%)	21 (18%)
Gleason pattern 4	40	0	2 (5%)	14 (35%)	24 (60%)
Metastatic cancer	1	0	0	0	1 (100%)

[a]Semiquantification of immune-labeling intensity in tissue microarrays.

Immunohistochemical staining of Trx1 was semiquantitatively graded as negative (-), weak (+), moderate (++), or strong (+++) staining in at least 50% of cells examined. The relationship between the intensity of Trx1 staining, primarily in the nucleus, and prostate cancer stages were analyzed ($p<0.01$).